ELSEVIER

Catalysis Today 36 (1997) 273–284

CATALYSIS TODAY

Supported phosphonate–phosphane complexes for vapour-phase carbonylation

Stefan Bischoff *, Axel Weigt, Michael Kant, Ulrich Schülke, Bernhard Lücke

Institute for Applied Chemistry Berlin-Adlershof, Rudower Chaussee 5, D-12489 Berlin, Germany

Abstract

Supported mixed bidentate rhodium and iridium complexes derived from phosphonate–phosphanes were studied in the methanol carbonylation and in the hydroformylations of ethylene and propylene. Heterobidentate complexes of rhodium showed higher activities than rhodium bisphosphane complexes in homogeneous and vapour-phase methanol carbonylation. The hemilabile behaviour of the mixed bidentate complexes may explain these findings. In ethylene hydroformylation, supported phosphonate–phosphane Rh-complexes did not show higher activities than supported rhodium–bisphosphane complexes. However, phosphonate–phosphane ligands suppressed the undesired ethane formation in this reaction. Excellent rhodium catalysts for vapour-phase carbonylations were obtained, when Rh phosphane complexes were anchored in lamellar zirconium phosphonate structures with mixed phosphonate anions. These catalysts were several times more active than rhodium supported on silica or on activated carbon, showed a superior stability, and produced butyraldehydes with up to 98% chemoselectivity in the vapour-phase hydroformylation of propylene.

Keywords: Vapour-phase carbonylation; Supported rhodium catalysts; Phosphonate–phosphane complexes; Zirconium phosphonate catalysts

1. Introduction

Phosphonate–phosphanes, which have a P- and an O-coordinating group, belong to the class of mixed bidentate ligands. Other compounds of this class, such as ether–phosphanes [1–4], phosphane oxide–phosphanes [5,6], phosphano–pyridines, and phosphano–amines [7,8] are known to enhance activities or selectivities of Rh-catalysed carbonylations. It has been suggested that the weakly coordinating group of the bidentate ligand changes between a coordinated and an uncoordinated state during the catalytic cycle, thus forming chelate and open-chain metal complex structures [1–5]. This phenomenon has been referred to as hemilabile behaviour. The intramolecular generation and occupance of free coordination sites has been assumed to accelerate rate determining steps in methanol carbonylation [4,5] and other reactions [9–11]. Mixed bidentate ligands do not necessarily form hemilabile complexes. No evidence for hemilabile behaviour was found for the phosphane sulphide–phosphane $Ph_2PCH_2P(S)Ph_2$. This ligand was reported to form a rhodium catalyst that is eight times more active in methanol carbonylation than the conventional Monsanto-catalyst [12].

We investigated phosphonate–phosphanes, because these heterobidentate ligands can form

* Corresponding author.

PII S0920-5861(96)00228-3

hemilabile Rh complexes [13]. A methanol carbonylation cycle with phosphonate–phosphane Rh intermediates in different coordination and oxidation states is suggested in Scheme 1. In this cycle, the ring-opening of phosphonate–phosphane Rh^{I} complexes should facilitate the formation of free coordination sites for the rate-determining oxidative addition of methyl iodide, while O,P-chelates should stabilise the more oxyphilic Rh^{III}-intermediates. Chelate structures were assumed to play a role in determining the rate of the carbonylation and this has been confirmed by the effects of the distance between the phosphane and the phosphonate group on the activation enthalpies [14].

To find out how phosphonate–phosphane ligands influence carbonylations with other rate-determining steps than the oxidative addition of an alkyl halide, we investigated the hydroformylations of ethylene and propylene using Rh-complexes adsorbed on activated carbon. The dialkyl phosphonate groups of the ligands are not assumed to be chemically bound to the surface of this support. Phosphonate–phosphanes and their Rh complexes were also anchored in the lamellar matrices of α-zirconium phosphonates to study catalysts with chemically

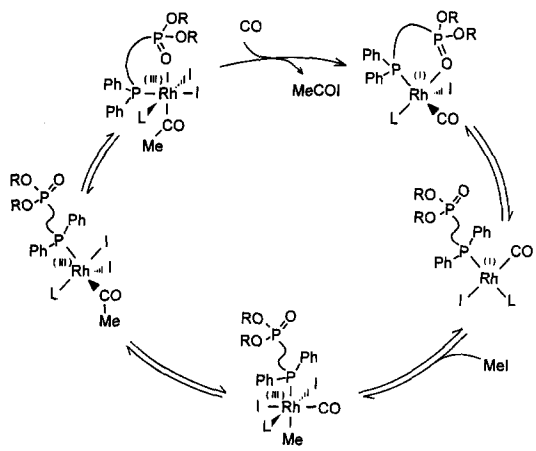

Scheme 1. Suggested catalytic cycle for the carbonylation of methanol catalysed by hemilabile phosphonate–phosphane rhodium complexes (Ph = C_6H_5, Me = CH_3, R = CH_3, $^{i}C_3H_7$; L = CO, I, phosphane). The promoter methyl iodide is in equilibrium with methanol and HI, the last being released from the irreversible reaction of acetyl iodide with methanol or water.

fixed phosphane ligands. Zirconium phosphonates with mixed phosphonate anions — in the following referred to as mixed zirconium phosphonates — can be prepared by co-precipitation of mixtures of phosphonic acids with Zr^{IV} compounds and are known to form amorphous, semicrystalline and crystalline layered structures [15–19]. The interlayer distance can be varied by suitable inorganic or organic pillars. The idea of anchoring phosphanes via covalently bound phoshonate groups in the layers of zirconium phosphonates is not new [20,21]. For their modification with phosphane groups, the presence of free phosphonic acid phosphanes is required. As yet, silyl esters of phosphonic acid–phosphanes have been used for an in-situ hydrolysis to form the free acid. During the preparation of the bis-(trialkyl silyl) esters, the alkylation of phosphane groups and, thus, the loss in transition metal-coordinating groups cannot be excluded. Recently, we developed new procedures to prepare pure phosphonic acid–phosphanes avoiding phosphane alkylation [22]. Therefore, the occurrence of alkylated phosphane groups can be excluded in our mixed zirconium phosphonate catalysts. Some features of these rhodium-containing organic–inorganic composite catalysts in the vapour-phase hydroformylation of propylene are reported on in the present work.

2. Experimental procedures

Phosphonate–phosphanes $(RO)_2P(O)–X–PPh_2$ **1a** and **1b**, **a**: X = CH_2, R = ^{i}Pr, **b**: X = $(CH_2)_2$, R = Me, were employed to prepare the open-chained rhodium complexes [ClRh(cod)**1a**] = **2a** (cod = 1,5-cyclooctadiene) and [ClRh(cod)**1b**] = **2b** as previously described [13]. Supported catalysts for vapour-phase carbonylations were prepared by impregnation of activated carbon (Desorex ED47, Lurgi, 800 m^2/g) and silica (Alfa Products, 270m^2/g, main pore diameter: 12 nm) with **2a**, **2b**, $[ClRh(cod)]_2$,

[ClRh(CO)(dppe)] (dppe = Ph_2P–$(CH_2)_2$–PPh_2), [ClRh(cod)(dppe-O)] (dppe-O = Ph_2P–$(CH_2)_2$–$P(O)Ph_2$), $[(dppp)Rh(CO)Cl]_2$ (dppp = Ph_2P–$(CH_2)_3$–PPh_2), and $Rh(OAc)_2$ dissolved in methylene chloride or with aqueous solutions of $RhCl_3$. We precipitated mixed zirconium phosphonates according to reference [15] from aqueous solutions of $ZrOCl_2$ and from ethanol/water (20/80 vol.%) solutions of $CH_3PO_3H_2$, H_2O_3P–$(CH_2)_6$–PO_3H_2, o-$[(C_6H_5)_2P]C_6H_4CH(OH)$–$PO_3H_2$ = **1c** [22], and [Rh(cod)(acac)]. To obtain a higher crystallinity, the precipitation was followed by treatment with hydrofluoric acid [22] in several cases. Silicagels loaded with 25 to 50 wt.% of mixed zirconium phosphonates were prepared by the reaction of $ZrOCl_2 \cdot 8H_2O$ with mixtures of $CH_3PO_3H_2$, H_2O_3P–$(CH_2)_6$–PO_3H_2, and **1c** within the mesopores of the silica (270 m^2/g, main pore diameter: 12 nm). The treatment of these materials with solutions of (cod)Rh(acac) or (acac)$Rh(CO)_2$ in methylene chloride at room temperature for 4 h and with hydrofluoric acid resulted in yellow catalysts [22], which were used without any further activation procedure. The total metal loading of the supported complex catalysts varied between 0.4 and 2 wt.%. N_2-adsorption/desorption measurements were conducted with a Gemini III 2375 surface area analyzer (Micromeritics Instruments). In-situ IR-investigations were carried out with 20–50 mg of self-supporting catalyst tablets in a quartz cell. The transmission spectra were recorded with a BIORAD FTS 60A-FTIR-spectrometer. In order to make comparisons, the spectra were related to those of pure silica or in the case of CO-adsorption to the starting spectrum. The spectra of the pure substances $[ClRh(cod)]_2$, **1b**, **2b**, dppe, [ClRh(CO)(dppe)] in KBr were employed to interpret the spectra of the supported complexes.

A continuous flow type reaction apparatus with a fixed bed was used for the vapour-phase carbonylations. The catalysts (400–600 mg) were investigated without any activation procedure. The reactor (made of a stainless steel tube with an inner diameter of 6 mm and provided with an inserted thermocouple) was heated to the desired reaction temperature in an Ar-stream under atmospheric pressure. CO or syngas was fed to build up the reaction pressure between 0.2 and 2 MPa, which was set with a back-pressure regulator. The flow-rates of gaseous reactants were adjusted with mass-flow controllers. Methanol and methyl iodide were introduced with a Shimadzu LC 10AD HPLC pump and evaporated in a pre-heated tube. Product gas analysis was conducted with an on-line gas chromatograph (1 m × 3 mm Porapack N or 25 m × 0.053 mm Poraplot Q) equipped with a sampling valve and a flame ionization detector. If not otherwise stated, catalytic runs were carried out under the following conditions: methanol carbonylation: 180°C, 2MPa, W/F = 2 g-cat · h/mol, CO/MeOH/MeI molar ratio 100/19/1; ethylene hydroformylation: 140°C, 2MPa, W/F = 5 g-cat · h/mol, $CO/H_2/C_2H_4$ molar ratio 2/2/1; propylene hydroformylation: 0.5MPa, W/F = 3 g-cat · h/mol, $CO/H_2/C_3H_6$ molar ratio 2/2/1.

3. Results and discussion

3.1. Methanol carbonylation

We have previously reported [14] that the open chained phosphonate–phosphane–rhodium complexes such as **2a** or **2b** can easily be converted into chelate structures, that the phosphoryl–oxygen is coordinated to the rhodium in the chelate structures, that **2a** and **2b** are excellent catalyst precursors in homogeneous methanol carbonylation, that the reaction order of the promoter methyl iodide decreases from 1 to 0.5 in the presence of **1a** and that the activation enthalpies increased with growing distance between the strongly coordinating phosphane group and the weakly coordinating phosphonate group. We suggested that the soluble phosphonate–phosphane–rhodium complexes work as hemilabile catalysts, as illustrated in Scheme 1.

Alkyl phosphonates are generally known as alkylating reagents. In the absence of methyl iodide, the phosphonate–phosphane complexes **2a** and **2b** did not show any activity, not even, when the corresponding ligands **1a** or **1b** were added to reach ligand:rhodium molar ratios of up to 10:1. Therefore, we can exclude the possibility that the phosphonate groups in the proximity of rhodium work as alkylating reagents to enhance the formation of rhodium–methyl species.

Although **1b** and the dimer $[ClRh(cod)]_2$ react smoothly at room temperature to form **2b** [13], subsequent co-impregnation of activated carbon with the phosphonate–phosphane and $[ClRh(cod)]_2$ did not result in catalysts with higher activities than $[ClRh(cod)]_2$ deposited alone on activated carbon. Subsequent co-impregnation does not guarantee the formation of phosphonate–phosphane rhodium complexes. On the other hand, when complex **2b** was impregnated on activated carbon, rate enhancements were observed in the vapour-phase carbonylation of methanol. This is an indication of the persisting coordination of the phosphonate–phosphanes to rhodium centres under vapour-phase carbonylation conditions. Fig. 1 displays carbonylation activities for several rhodium complexes supported on activated carbon. Dimethyl ether was found as the major by-product under the conditions we applied to keep the conversions below 10%. Its selectivity decreased with increasing methanol conversion. The phosphane oxide–phosphane dppe-O, which is known to accelerate the homogeneous carbonylation [5], did not improve the activity of the carbon-supported catalyst. Strongly coordinated chelate ligands (dppe) can even decrease the activity, possibly by blocking coordination sites necessary for the carbonylation. The activity enhancement by the phosphonate–phosphane ligands **1a** and **1b** is obvious. However, uniform activation energies of about 30 kJ/mol were found for the supported complexes $[ClRh(cod)]_2$, [ClRh(CO)(dppe)], **2a** and **2b**. Decreasing carbonylation activities were observed when argon was added to increase the total pressure (Fig. 2). This means that the diffusion of reactants influences the observed rates. Therefore, the observed activation energies cannot be used to discuss the hemilabile behaviour of the supported complexes as done with the corresponding soluble catalysts [14].

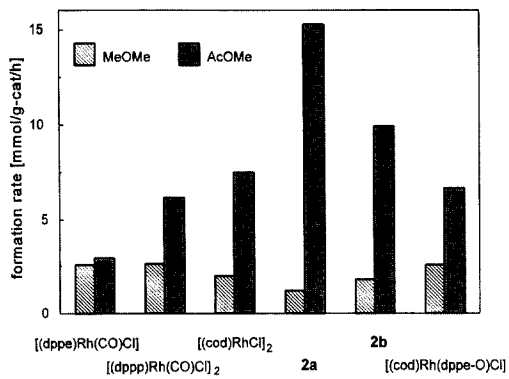

Fig. 1. Ligand effects on the methanol carbonylation activity of rhodium complexes supported on activated carbon; reaction conditions: metal loading 0.5 wt.% Rh, 180°C, 2 MPa, W/F = 2 g-cat·h/mol, CO/MeOH/MeI molar ratio = 100/19/1.

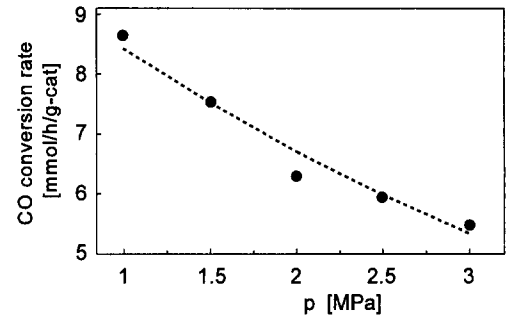

Fig. 2. Influence of the total pressure on the carbonylation rate of $[ClRh(cod)]_2$ supported on activated carbon; reaction conditions: metal loading 0.5 wt.% Rh, 180°C, $W/F_{CO+MeOH+MeI}$ = 2 g-cat·h/mol, Ar/CO/MeOH/MeI molar ratio = X/50/19/1 with X = 0, 35, 70, 105, 140; the total pressure was varied by changing only the partial pressure of Ar.

The formation of $Rh^{I}(CO)_2^+$ dicarbonyl-species in the presence of CO, as displayed in Fig. 3, shows that two coordination sites can easily be substituted in the cases of $[ClRh(cod)]_2$ and **2b** supported on silica. The chelating bis-phosphane–ligand dppe is significantly harder to substitute with CO. This fact fits well to-

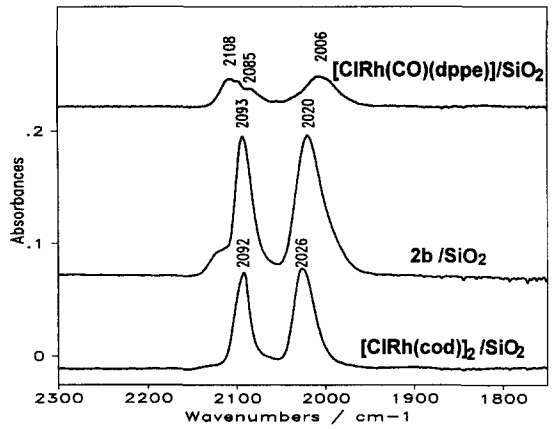

Fig. 3. FTIR spectra of [ClRh(CO)(dppe)], **2b** (= [ClRh(cod)(Ph_2P–$(CH_2)_2$–P(O)$(OMe)_2$)]) and [ClRh(cod)]$_2$ after their impregnation on silica, subsequent treatment with CO at 150°C and evacuation at room temperature.

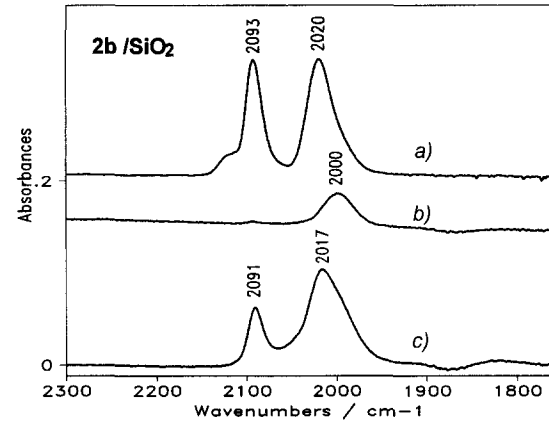

Fig. 5. FTIR spectra of **2b** (= [ClRh(cod)(Ph_2P–$(CH_2)_2$–P(O)$(OMe)_2$)]) after the following sequence of treatments: a) impregnation on silica, chemisorption of CO at 150°C, evacuation at room temperature, b) evacuation of the sample at 250°C and c) chemisorption of CO at 150°C, evacuation at room temperature.

gether with the decreased carbonylation rate on the supported dppe complex. The hemilabile ligand **1b** stabilises supported rhodium monocarbonyl species even at the elevated temperature at which decarbonylation occurs on the other supported rhodium catalysts (Fig. 4). The decarbonylation creates coordinatively unsaturated sites which could be stabilised by coordinating the phosphonate groups. The monocarbonyl species with their remarkable thermal stability can be partly reconverted into dicarbonyl-species even at higher temperatures

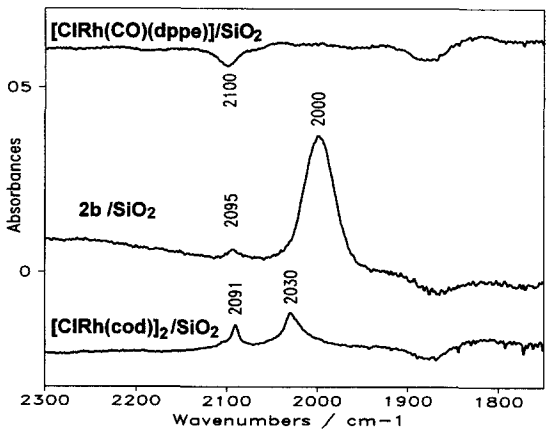

Fig. 4. FTIR spectra of silica-supported [ClRh(CO)(dppe)], **2b** (= [ClRh(cod)(Ph_2P–$(CH_2)_2$–P(O)$(OMe)_2$)]) and [ClRh(cod)]$_2$ after treatment with CO at 150°C and evacuation at 250°C.

by increasing the CO partial pressure (Fig. 5). The above findings support the idea that the phosphonate–phosphane complexes may also form supported hemilabile catalysts. IR studies by other authors [23] suggest that the mechanisms of homogeneous and heterogeneous methanol carbonylation do not differ essentially when rhodium salts are deposited on silicagel. However, catalysts prepared by the impregnation of silica with **2b**, [ClRh(cod)]$_2$ and [ClRh(CO)(dppe)] deactivated after several hours in the vapour-phase carbonylation of methanol, making steady-state investigations with these catalysts impossible. In contrast, activated carbon gave catalysts which were stable over several days.

The suggestion that the hemilabile O,P-ligands enhance changes in the oxidation states of intermediates implies that increased rates cannot be expected when these changes do not occur in rate-determining steps. The last premise is true for supported iridium catalysts, where the oxidative addition of methyl iodide proceeds much faster than the methanolysis of acetyl species [24]. The rate-determining methanolysis of iridium acetyl species does not change the formal oxidation state of iridium. Accordingly, the hemilabile ligands did not increase the car-

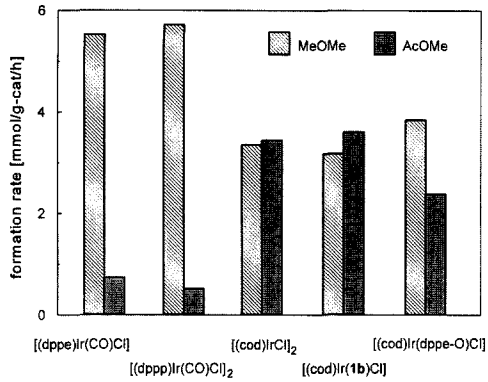

Fig. 6. Ligand effects on the methanol carbonylation activity of iridium complexes supported on activated carbon; reaction conditions: metal loading 0.5 wt.% Ir, 180°C, 2 MPa, W/F = 2 g-cat·h/mol, CO/MeOH/MeI molar ratio = 100/19/1.

bonylation activity of iridium complexes supported on activated carbon (Fig. 6). The inhibition effect of chelating ligands like dppe and dppp is more significant for the iridium catalysts than for the corresponding rhodium catalysts.

3.2. Hydroformylation

Ligand effects were also observed in the vapour-phase hydroformylation of ethylene on rhodium complexes supported on activated carbon (Fig. 7). Ethane, propionaldehyde and diethyl ketone were obtained as products, as also reported in reference [25]. Both ligands, dppe and **1b** promoted the activity. This is in contrast to the vapour-phase carbonylation of methanol. Hemilabile behaviour of phosphonate–phosphane complexes does not seem to play a role in the hydroformylation of ethylene, since the strongly chelating ligand dppe also enhanced the total activity. The selectivity of the hydrogenation product ethane was nearly doubled by the chelating ligand dppp, while the phosphonate–phosphanes diminished the selectivity of ethane. The ethylene hydroformylation route requires one more free coordination site than the hydrogenation of ethylene, where CO-chemisorption and insertion are not required. Based on observations we made during the preparation of **2a** and **2b** [13], the phosphonate–phosphanes are assumed to function as monodentate ligands under the applied conditions and to provide free coordination sites for the hydroformylation pathway more easily than chelating ligands do. This would explain the observed higher selectiv-

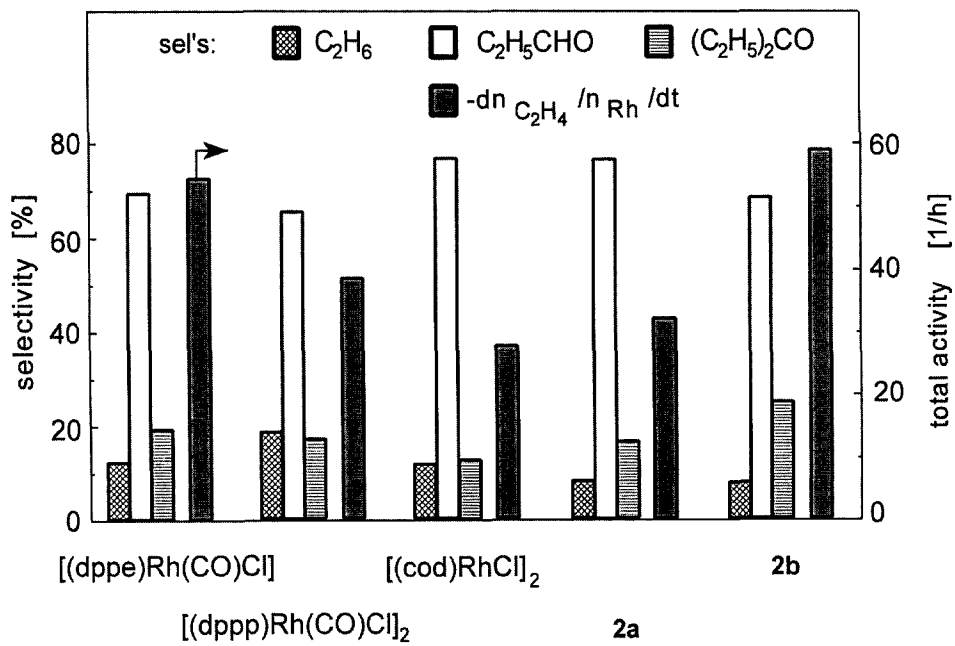

Fig. 7. Ligand effects on the hydroformylation of ethylene catalysed by rhodium complexes supported on activated carbon; reaction conditions: metal loading 0.5 wt.% Rh, 0.6 g cat., 140°C, 2 MPa, W/F = 5 g-cat · h/mol, $CO/H_2/C_2H_4$ molar ratio = 2/2/1.

ities of oxygenates over supported **2a** and **2b**. All the complexes supported on activated carbon showed activity declines of 10 to 30% in the vapour-phase hydroformylation after three days on stream.

Silica can be surface-modified with phosphanes to coordinate catalytically active rhodium clusters. Such catalysts have been reported to show high chemoselectivities in the vapour-phase hydroformylations of ethylene and propylene [26,27]. While silica is an amorphous support material, zirconium phosphonates can form stable crystalline layered structures, which can be varied over a wide range. It has been reported that the regioselectivity in the hydroformylation of allyl alcohol was changed by intercalation of the catalytically active rhodium complex in montmorillonite [28]. Such effects are also expected for layered zirconium phosphonates. Furthermore, these offer a rich potential for their modification with functional groups, for the intercalation of transition metal complexes and for the creation of specific surroundings of the catalytic centres. As yet, the limited availability of phosphanes with phosphonic acid groups seems to have slowed down the development of phosphane complex catalysts intercalated between the layers of zirconium phosphonates. Mixed phosphonate catalysts have already been successfully used in slurry-phase hydroformylation [20,21]. To prevent rhodium-leaching, probably caused by its insufficient coordination, the layered zirconium phosphonate catalysts, containing the intercalated rhodium were treated with long-chained bisphosphonic acids. The isomorphic substitution of phosphonate groups at the edges of the crystallites with the above bisphosphonic acids was claimed to have produced "jail-celled" or "bird-cage" catalysts. Significant amounts of the quaternised phosphane $H_2O_3P–C_2H_4–P(Me)Ph_2]^+I^-$ were obtained in our attempts to prepare $H_2O_3P–C_2H_4–PPh_2$ according to reference [21]. To avoid the undesired alkylation of phosphane groups, we used phosphanes with covalently bound phosphonic acid groups, for example o-$[(C_6H_5)_2P]C_6H_4CH(OH)–PO_3H_2$(**1c**) for the precipitation of the catalyst precursors (Scheme 2).

Mixed zirconium phosphonates with the formula $Zr(O_3PCH_3)_x(O_3PC_6H_{12}PO_3)_y$(**1c**)$_z$, $(x + 2y + z = 2)$, were used as organic–inorganic polymer ligands for the catalytically active rhodium. BET-surface areas between 50 and 400 m^2/g were found for the materials. As yet, have not clarified whether the mixed phosphonates form staggered layers, as recently discussed by Clearfield et al. [15]. However, mixed zirconium phosphonate catalysts, precipitated from solutions of $ZrOCl_2$ and of $CH_3PO_3H_2$, $H_2O_3P–(CH_2)_6–PO_3H_2$, **1c** and [Rh(cod)(acac)], showed good stabilities over several days and high aldehyde selectivities in the vapour-phase hydroformylation of propylene. Fig. 8 compares the propylene conversion rates and the selectivities over rhodium catalysts supported on silica, activated carbon and $Zr(O_3PCH_3)(O_3PC_6H_{12}PO_3)_{0.25}$(**1c**)$_{0.5}$ at 160°C. Significantly higher activities and excellent aldehyde selectivities compared to those of the supported metal catalysts, indicate that complex catalysis occurs in the zirconium phosphonate catalysts. Butyraldahyde selectivities of about 94%, (linear/branched = 2.7/1 to 3.5/1), propane selectivities lower than 4% and a propylene conversion rate of 19 $mol/mol_{Rh}/h$ (Rh/SiO_2: 0.6 $mol/mol_{Rh}/h$, Rh/activated carbon: 4.8 $mol/mol_{Rh}/h$) have been observed at 100°C. Fig. 9 illustrates the different behaviour of a supported rhodium metal catalyst and a zirconium phosphonate — rhodium catalyst during the first hours on stream, in which the temperature was increased stepwise after several hours. Rhodium supported on activated carbon showed declines in activity at all the temperatures. Active centres for butanol formation were generated at 190°C, while the decrease in propylene hydroformylation and hydrogenation progressed. Propane was not a minor product at temperatures above 160°. In contrast, beginning at 130°C, an activation process occurred with the zirconium phosphonate–

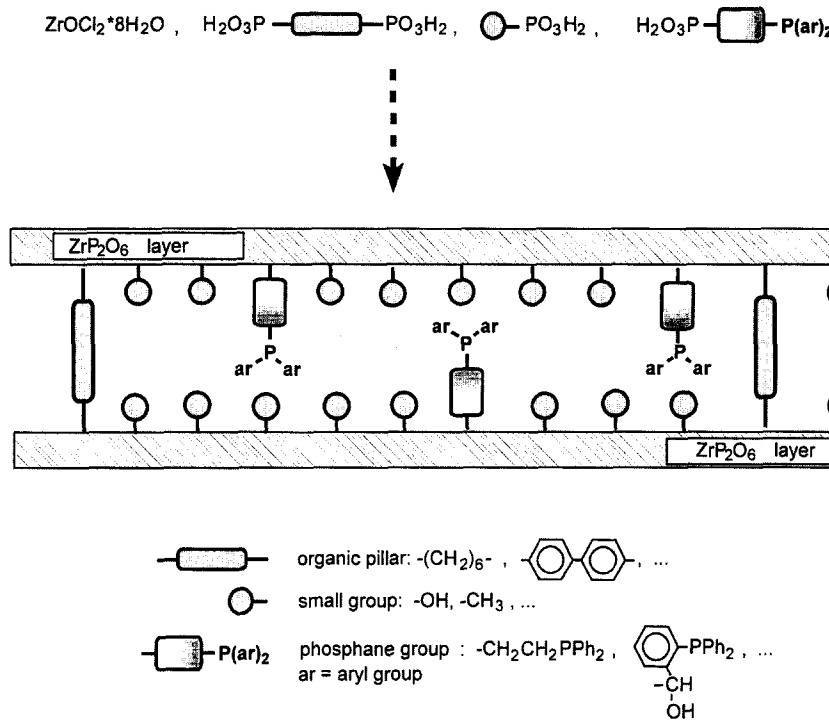

Scheme 2. Model for the zirconium phosphonate structures prepared with phoshonic acid–phosphanes.

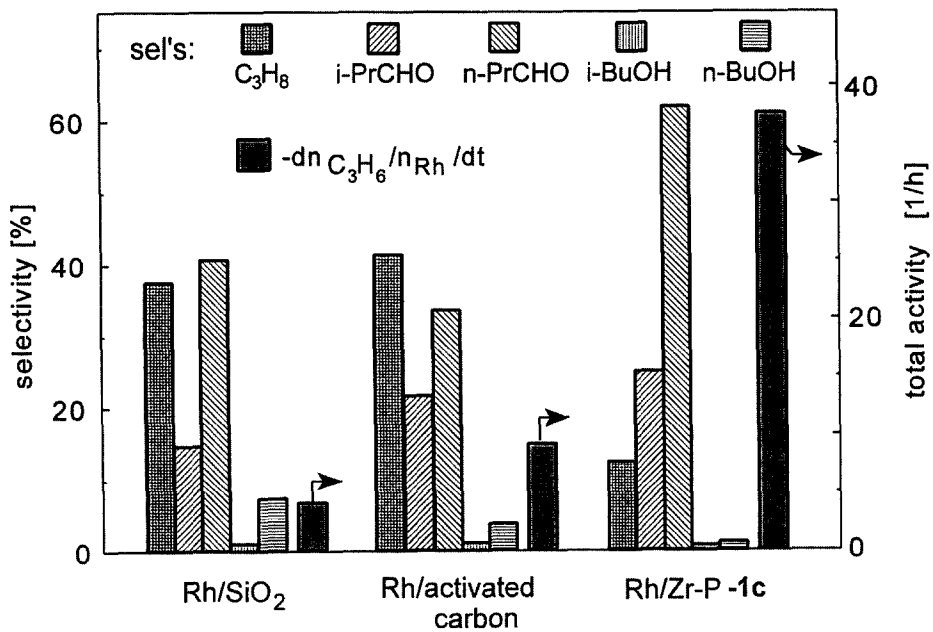

Fig. 8. Hydroformylation of propylene on supported rhodium metal and rhodium complex catalysts; reaction conditions: 0.8 wt.% Rh/SiO_2, 2 wt.% Rh/activated carbon, 0.8 wt.% Rh/Zr–P–**1c** = $Zr(O_3PCH_3)(O_3PC_6H_{12}PO_3)_{0.25}$(**1c**)$_{0.5}$, 160°C, 0.5 MPa, W/F = 3 g-cat · h/mol, $CO/H_2/C_3H_6$ molar ratio = 2/2/1.

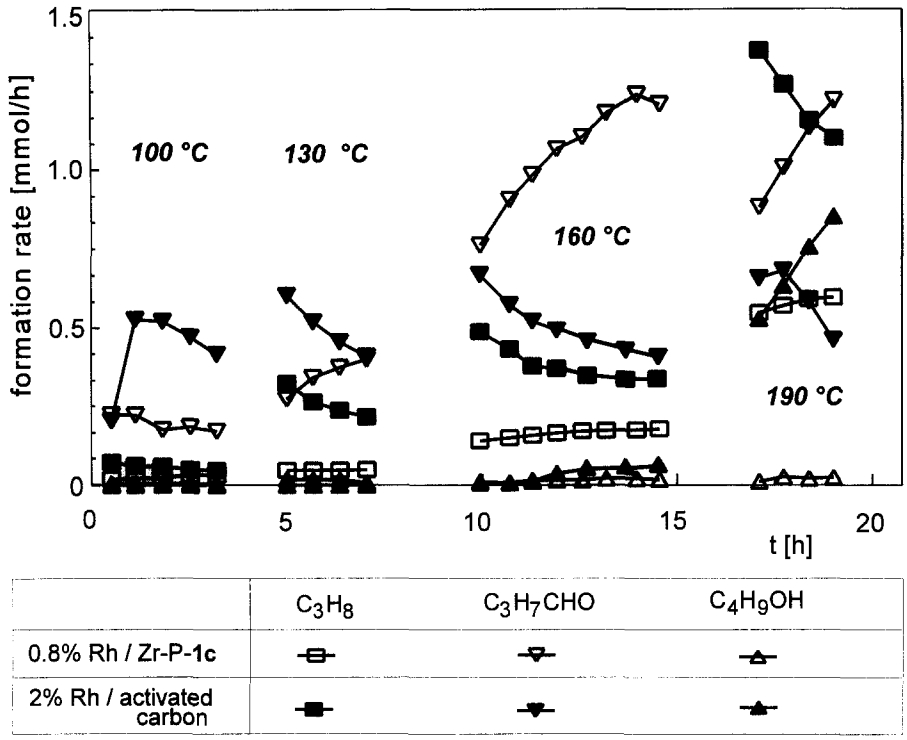

Fig. 9. Activity changes in the hydroformylation of propylene over 2 wt.% Rh/activated carbon and 0.8 wt.% Rh/Zr–P–**1c**; reaction conditions: 0.5 MPa, W/F = 3 g-cat · h/mol, $CO/H_2/C_3H_6$ molar ratio = 2/2/1.

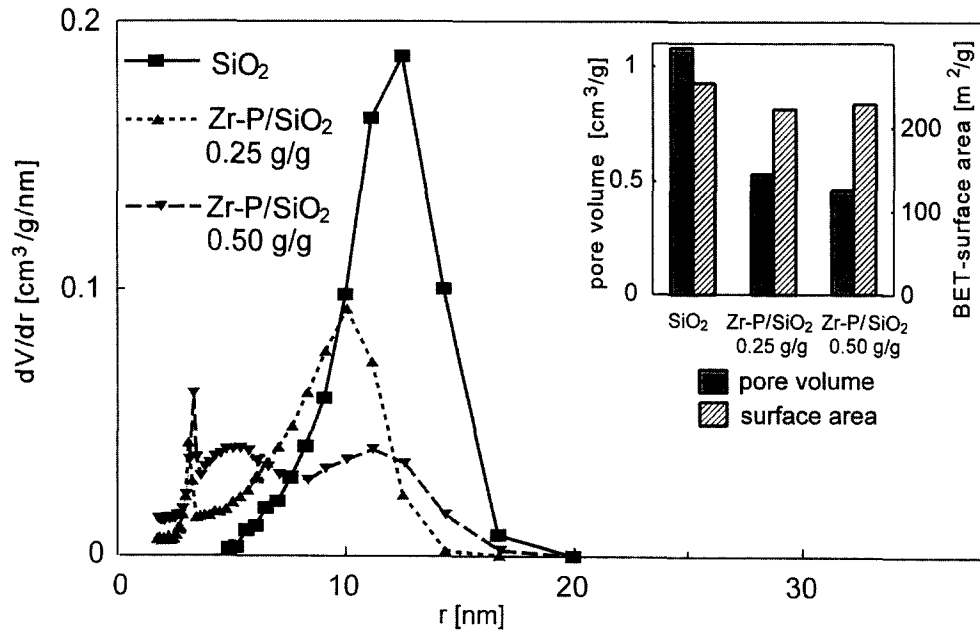

Fig. 10. Pore volume distributions, pore volumes and BET surface areas of silica and silica loaded with zirconium phosphonates. The mass fraction of the zirconium phosphonate is related to the total mass of the composite.

rhodium catalyst which continued even at 190°C where the metal catalyst deactivated. It is interesting that all the zirconium phosphonate–rhodium catalysts were at least two times more active at 100°C after the stepwise temperature increase than before. The fact that the selectivities were as good as before this treatment demonstrates the high thermal stabilities of the catalysts.

Interlayer distances usually ranging from 7 to about 20 Å imply that diffusion of reactants and products could decrease the activity. We tried to precipitate the zirconium phosphonate catalysts within the pores of a mesoporous carrier to obtain a bimodal catalyst with mesopores for a smooth mass transfer and micropores for the reaction sites. A mesoporous carrier was chosen to restrict the size of layered structures to the pore diameters. As visible from the pore volume distribution plots in Fig. 10, we succeeded in filling about half of the mesopore volume of the silicagel with zirconium phosphonate catalyst structures. The small sharp peak at 35Å is typical for these structures. As expected, the pore volume distribution shifted to smaller pores with increasing zirconium phosphonate loading, while the BET surface area did not significantly change. The catalyst with the formula $Zr(O_3PCH_3)(O_3PC_6H_{12}PO_3)_{0.33}$(**1c**)$_{0.34}$ containing 0.8 wt.% Rh showed formation rates for propane, iso- and n-butyraldehyde of 0.8, 4.1, and 17.0 mol/mol$_{Rh}$/h at 100°C after the above mentioned stepwise temperature increase. When the same rhodium-containing mixed zirconium phosphonate was prepared within the mesopores of silica, a composite catalyst with both mesopores and micropores was formed. At 100°C, propane, iso- and n-butyraldehyde were formed with rates of 2.4, 42.1, and 58.1 mol/mol$_{Rh}$/h on this catalyst. This remarkable activity improvement confirms the above concept of enhanced activity on bimodal catalysts. The low propane selectivity of 2.4% over the composite catalyst strongly suggests that the active metal does not form silica-supported metal particles, which would lead to propane selectivities above 30%. It is assumed that this catalyst also works as a supported rhodium complex catalyst, for which low alkane selectivities are typical [26,27].

Table 1
Reaction orders in the hydroformylation of propylene over mesoporous silica modified with a zirconium phosphonate rhodium catalyst [a] according to the rate law $r_i = k_i \cdot p^m_{C_3H_6} \cdot p^n_{H_2} \cdot p^q_{CO}$ [b]

	Reaction orders of		
	C_3H_6	H_2	CO
product i	***m***	***n***	***q***
C_3H_8	0.1	0.7	−0.2
i-C_3H_7CHO	0.1	1.2	0.6
n-C_3H_7CHO	0.2	1.2	0.4

[a] 0.4wt.% Rh/$Zr(O_3PCH_3)(O_3PC_6H_{12}PO_3)_{0.25}$(**1c**)$_{0.5}$/$SiO_2$, $m_{Zr-P\ catalyst}/m_{silica} = 0.5$.
[b] r_i: formation rate for product i; k_i: rate constant; p: partial pressure; m, n, q: reaction orders; propylene conversion was kept below 10%.

Table 1 shows reaction orders in the vapour-phase hydroformylation of propylene on the composite catalyst. The values of about 1 for H_2 indicate that the hydrogenolysis of acyl species is a rate-determining step. Rate-limiting hydrogenation of adsorbed acetyl species was also reported for ethylene hydroformylation over silica-supported rhodium catalysts [29]. As expected, CO suppresses the hydrogenation route in which propane is formed. The orders of about 0.5 found for CO suggest that its insertion is another rate-limiting step. Olefin insertion does not seem to determine the rate, as the low reaction orders of propylene suggest. Different reaction orders for CO and the olefin were found in the hydroformylation of ethylene over activated carbon-supported and silica-supported rhodium metal catalysts [25,29]. The reaction orders for CO of −1 and −0.4 respectively show that CO can even inhibit the hydroformylation. Furthermore, reaction orders of about 1 for ethylene indicate that the olefin is involved in a rate limiting step of the hydroformylation over the supported metal catalysts. The comparison of the reaction orders in Tab. 1 with the above-mentioned data suggests that the mixed zirconium phosphonate rhodium catalysts do not work as supported metal catalysts.

It should be noted that the composite catalysts made of mesoporous silica and zirconium phosphonates in some cases showed declines of up to 50% in their activity after 5 days on stream. Although X-ray diffraction spectra showed the existence of semicrystalline zirconium phosphonate phases, we could not yet clarify whether the hydroformylation occurs mainly in the interlayer regions or in outer surface areas or on films of this material on silica.

4. Conclusions

Phosphonate–phosphanes, as presented in this work, are interesting ligands for carbonylation catalysts based on rhodium. Activated carbon is the support of choice for adsorbing rhodium complexes with mixed bidentate ligands. Hemilabile complexes were only superior in the rhodium-catalysed carbonylation of methanol, but not in the iridium-catalysed methanol carbonylation and also not in the vapour-phase hydroformylation of ethylene. Hemilabile behaviour of the O,P-ligands seems to enhance carbonylations only when it occurs in rate-determining steps in which oxyphilic intermediates are formed. This condition is fulfilled in the rhodium-catalysed carbonylation of methanol, where the oxidative addition of methyl iodide to Rh^{I} species produces oxyphilic Rh^{III} species.

Mixed zirconium phosphonates modified with phosphanes which are covalently bound to the inorganic matrix, can provide active rhodium catalysts for the vapour-phase hydroformylation of propylene. They are several times more active than rhodium metal catalysts supported on silica or on activated carbon, show superior stabilities, and produce butyraldehydes with up to 98% chemoselectivity. The experimental findings strongly suggest that the vapour-phase hydroformylation over the presented rhodium-containing mixed zirconium phosphonates is catalysed by rhodium complexes. Further work is necessary to characterise the layer structures and catalytic centres, to improve the mechanical stability and to evaluate further applications in slurry-phase carbonylations of substrates with lower vapour pressures.

Acknowledgements

The authors wish to thank Dr. H. Mießner for measuring and discussing FTIR spectra, Mrs. R. Jentzsch for catalyst preparations and Mrs. R. Dressel for numerous catalytic measurements.

References

[1] E. Lindner, H.A. Mayer and P. Wegner, Chem. Ber., 119 (1986) 2616.
[2] E. Lindner, A. Sickinger and P. Wegner, J. Organomet. Chem., 349 (1988) 75.
[3] E. Lindner, A. Bader, H. Bräunling and R. Jira, J. Mol. Catal., 57 (1990) 291.
[4] A. Bader and E. Lindner, Coordination Chem. Rev., 108 (1991) 27.
[5] R.W. Wegmann, A.G. Abatjoglou and A.M. Harrison, J. Chem. Soc., Chem. Commun., (1987) 1891.
[6] R.W. Wegmann and A.G. Abatjoglou, PCT Int. Appl. WO 8600888 (1986), CA, 105 (1987) 174788.
[7] C. Abu-Gnim and I. Amer, J. Mol. Catal., 85 (1993) L275.
[8] C. Abu-Gnim and I. Amer, J. Chem.Soc., Chem. Commun., (1994) 115.
[9] W.S. Knowles, Acc. Chem. Res., 16 (1983) 106.
[10] Z.M. Michalska, J. Mol. Catal., 19 (1983) 345.
[11] K.A. Ostoja Starzewski and J. Witte, Angew. Chem., 97 (1985) 610.
[12] M.J. Baker, M.F. Giles, A.G. Orpen, M.J. Taylor and R.J. Watt, J.Chem. Soc., Chem. Commun., (1995) 197.
[13] A. Weigt and S. Bischoff, Phosphorus, Sulphur, and Silicone, 102 (1995) 91.
[14] S. Bischoff, A. Weigt, H. Mießner and B. Lücke, J. Mol. Catal. A: Chemical, 107 (1996) 339.
[15] A. Clearfield, J. Don Wang, T. Ying, E. Stein and C. Bhardwaj, J. Solid State Chem., 117 (1995) 275, and references therein.
[16] G. Alberti, in C.A.C. Sequeira and M.J. Hudson, Eds., Multifunctional Mesoporous Inorganic Solids, Kluwer Academic Publishers, Dordrecht, 1993, p. 179, and references therein.
[17] A. Clearfield and B.D. Roberts, Inorg. Chem., 27 (1988) 3237.
[18] C. Ferragina, A. La Ginestra. M.A. Massucci, G. Mattogno, P. Patrono, P. Giannoccaro and M.Arfelli, J. Mater. Chem., 5 (1995) 461.
[19] J.A. Cusomano, in: J.M. Thomas and K.I. Zamaraev, Eds., Perspectives in Catalysis, IUPAC-Blackwell-Science Publications, Oxford, 1992, p. 1.

[20] M.B. Dines and P.M. DiGiacomo, Inorg. Chem., 20 (1981) 92.
[21] K.P. Callahan, P.M. DiGiacomo and M.B. Dines, Occidental Research Corp., US 4,386,013, 31.05.1983.
[22] M. Kant, S. Bischoff and U. Schülke, patent, submitted.
[23] J. Bódis, J. Zsakó, Cs. Németh and J. Mink, Vibrational Spectroscopy, 9 (1995) 197.
[24] G. Zehl, S. Bischoff and B. Lücke, Catal. Lett., 19 (1993) 247.
[25] N. Takahashi, Y. Sato, T. Uchiumi and K.Ogawa, Bull. Chem. Soc. Jpn., 66 (1993) 1273.
[26] T. Shido, T. Okkazaki, M.A. Ulla, T. Fujimoto and M. Ichikawa, Catal. Lett., 17 (1993) 97.
[27] T. Shido, T. Okkazaki and M. Ichikawa, J. Catal., 157 (1995) 436.
[28] K.N. Bhatt and S.B. Halligudi, J. Mol. Catal., 91 (1994) 187.
[29] M.W. Bakalos and S.S.C. Chuang, J. Catal., 151 (1995) 266.